Following of the Relaxations in a Polymer's Behavior Part I: "Correlation Diagram" and Creep at Linearly Increasing Temperature

J. M. GENEVAUX* and G. M. GUERRIN

LEMTA URA-875, 2 avenue de la forêt de Haye, 54504 Vandoeuvre, France

SYNOPSIS

The correlation diagram is introduced here in order to follow the different relaxations of polymers. Two examples will be presented: PMMA and wood at several moisture contents between 20 and 100°C. For the two materials, an experiment of creep at linearly increasing temperature is proposed, so as to point out the relaxations of the different components for low frequencies. In this experiment, a relaxation induces a maximum of creep kinetic. The movement of the temperatures of relaxation with the moisture content will be observed. For wood at high moisture content (near the fiber saturation point), the cellulose's relaxation of the reinforcements will be observed at high temperature.

INTRODUCTION

Creep or relaxation experiments, over a long time, are essential in order to understand the different behavior of a material. If this behavior depends on the temperature or the moisture content, these long-term experiments need a good regulation of the temperature and the hygroscopy of the atmosphere. In order to reduce the duration of the experiments, the behavior at higher temperature can be observed. If the equivalence time temperature is applicable at the tested material, the behavior at longer range can be deduced. In order to follow the relaxation of several mechanisms, a graph, called a correlation diagram, is proposed: the points $(1/T_0, \log f_0)$ for which the internal loss is maximum.

In the case of constant loads, a creep experiment at linearly increasing temperature is proposed (Part I). Thus, the relaxations of the successive mechanisms can be observed on a single sample. In the case of periodic loads, for frequencies near 1 Hz and 1 kHz quasistatic and dynamic experiments will be presented in the second part (Part II). They were obtained in bending using the double pendulum method ($\approx$ 1 Hz), and a forced vibration method in bending at the resonance of a double cantilever beam (1 kHz).

The results concern the polymethyl methacrylate (PMMA) and the wood (Douglas, Poplar) conditioned at several moisture contents. The effect of drying of wood should be avoided, so the maximum temperature in wood cannot exceed 100°C. The samples of PMMA, which are used to test the experimental techniques, were tested in the same experimental range.

CORRELATION DIAGRAM

Signature of a Mechanism

The different mechanical methods used to investigate the viscoelastic nonageing behavior permit the study of a large range of frequencies:

Ultrasounds	$10^5 \times 10^6$ Hz[1]
Resonance vibrations	$10^1 \times 10^4$ Hz[2]
Quasistatic	$10^{-1} \times 10^1$ Hz[2,3,4]
Low frequencies	$10^{-1} \times 10^{-4}$ Hz[5,6]
Creep and relaxation	$10^{-1} \times 10^{-8}$ Hz[7]

The temperature strongly influences the behavior of the polymer (amorphous and semicrystalline).

* To whom correspondence should be addressed.

Journal of Applied Polymer Science, Vol. 45, 1431–1439 (1992)
 CCC 0021-8995/92/081431-09$04.00

During a study at constant frequency, the increase in temperature induces an abrupt decrease of the apparent modulus at certain temperatures. These phenomena are called relaxation (Fig. 1). At a higher frequency, the relaxation temperatures are higher. The shift factor can also be deduced. For each mechanism, the line of the internal loss maxima, separates the behavior into two zones:

$$\text{Relaxed} \quad T > T_0$$
$$\text{Unrelaxed} \quad T < T_0$$

The vitrous transition of one of the components of the material appears as an important decrease of the apparent modulus (Fig. 1). It separates the vitrous state and the rubber state.[8,9]

Two Examples: PMMA and Wood

Several authors' results[1,5,10,11] allow us to draw the lines $(1/T_0, \log f_0)$ for the internal loss maxima, associated at the mechanisms of the PMMA [Fig. 4(a)]. The vitrous transition is located by the letter α. The second relaxation β (if we classify by order of amplitude of the decrease of the apparent modulus) is associated at the lateral ester groups. For a frequency near 1 Hz and at $T = 30°C$, the relaxation α' is superposed. It appears here that two relaxations, which do not have the same activation energy, can cross themselves in this diagram. Thus at this point, the internal friction is induced by the two mechanisms: Each cannot be observed separately. The water molecules are at the origin of the relaxation γ (0.95 Hz, −82°C), which is not visible on this part of the diagram.

An equivalent diagram can be built for different species of wood: here douglas (450 kg/m^3) and poplar (380 kg/m^3). In fact the behavior of the wood samples is governed by the three principal polymers of wood (Fig. 3): lignins ($\approx$ 25%), hemicellulose ($\approx$ 30%), and cellulose ($\approx$ 45%).[12] No distinctions have been made here between the two species: The weak differences of composition between softwood and hardwood do not appear clearly in the mechanical behavior. But it is necessary to take into account the moisture content H of the sample [Fig. 5(a)].

These graphs will be completed for very slow frequencies, owing to creep experiments at a linearly increasing temperature (Part I), and for frequency between 1 Hz and 1 kHz (Part II).

EXPERIMENTAL

Method

The short dimensions of the isostress samples (130 × 50 × 10 mm) (Fig. 2) allow the reduction of their thermical inertia and thus minimize the difference between the temperatures of the sample and the atmosphere. For a heating rate of 0.2°C/min, these differences are less than 1°C for the PMMA and depend on the moisture content of the wood (if $H \approx 30\%$, $\Delta T = -3°C$; if $H \approx 0\%$, $\Delta T = -2°C$). In the case of hygroscopic materials, it is necessary to follow the hygroscopic equilibrium curves in order to maintain a constant moisture content in the sample. The curves given by Kelwerth were used for wood.[13] A mass control, at the beginning and the end of the experiment, pointed out a decrease of the moisture content never greater than 3%. The deflection of the sample is measured every 5 min, at 60 mm of the fixed extremity. The loading is applied by weights. The palper induces a force of 1 N, which is neglected.

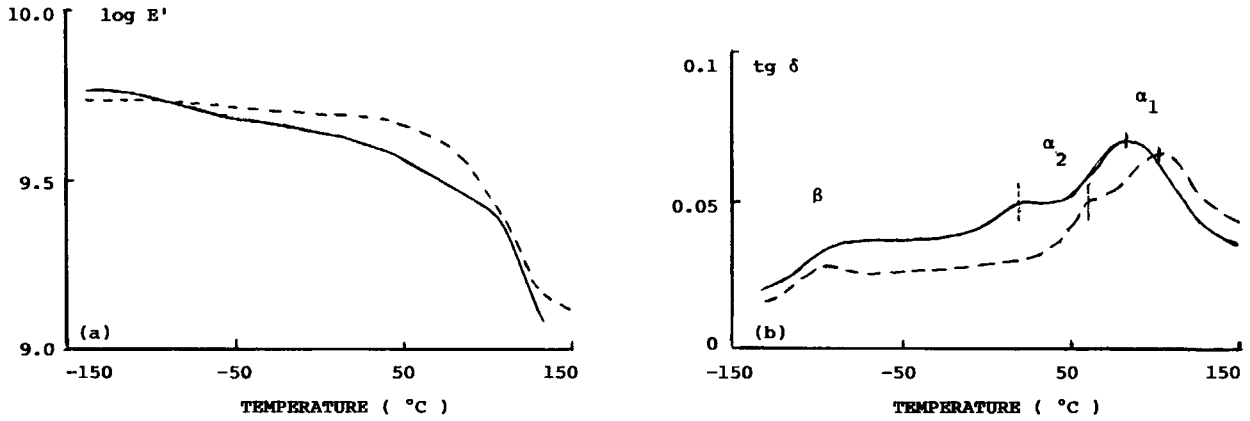

Figure 1 Comparison between the apparent modulus (E') et tan δ at a moisture content of 10%, for two species of wood. From Kelley.[3]

Table I Experimental Conditions and Moisture Content of the Samples

Sample	Load (N)	H before (%)	H after (%)
PMMA			
0	17.55	0.6	
1	17.57	0.6	
2	17.58	0.6	
3	17.80	0	
Douglas wood			
L_{30}	25.17	30.3	28.0
R_{30}	1.98	34.1	32.3
T_{30}	0.84	32.0	31.5
Douglas wood			
L_{10}	25.17	10.2	11.2
R_{10}	2.03	10.2	10.7
T_{10}	0.98	9.6	9.7
Poplar wood			
L_0	36.52	0	1.6
R_0	3.01	0	1.1
T_0	0.98	0	1.0

Conditioning

Samples of PMMA

In order to test the influence of the adsorbed water in the PMMA, four samples were prepared: two reference samples (Nos. 0 and 1); one sample immersed for 2 days (No. 2); and one sample dried at 105°C during 24 h (No. 3). A weight loss of 0.5% was observed.

They were cut from a plate of raw PMMA, obtained by the cyanhydrin aceton technique. No charges were added.

Wood Samples

The samples were cut at 20°C and 12% of moisture content. Due to the cylindrical orthotropy of the trunk, it was difficult to cut samples with a large tangential zone. The "most tangential zone" was placed between the measured point and the fixed extremity. In this case, the thinness of the sample induced only 1 or 2 annual rings in the thickness. One sample series was tested at $H \approx 10\%$ (L_{10}, R_{10}, T_{10}). Another was dried at 105°C during 24 h (L_0, R_0, T_0). The last series was immersed for 2 days and had a moisture content just below the fiber saturation point (L_{30}, R_{30}, T_{30}): All the water was contained by the cell wall, without free water in the cell lumen (Fig. 3).

Moisture Content Evaluation

After testing, each sample was dried in order to measure the moisture content during the experiment.

RESULTS

Figures 6 and 7 present the evolutions of the deflection versus time (or temperature: 5 mn $\approx$ 1°C). The deflection increase during 5 min [$v_f(t) = f(t) - f(t - 300s)$] was an approximation of the creep speed.

Samples of PMMA

The deflection of the two reference samples differed only by 1.5% after 6 h. The reproducibility was good when samples without variability were tested.

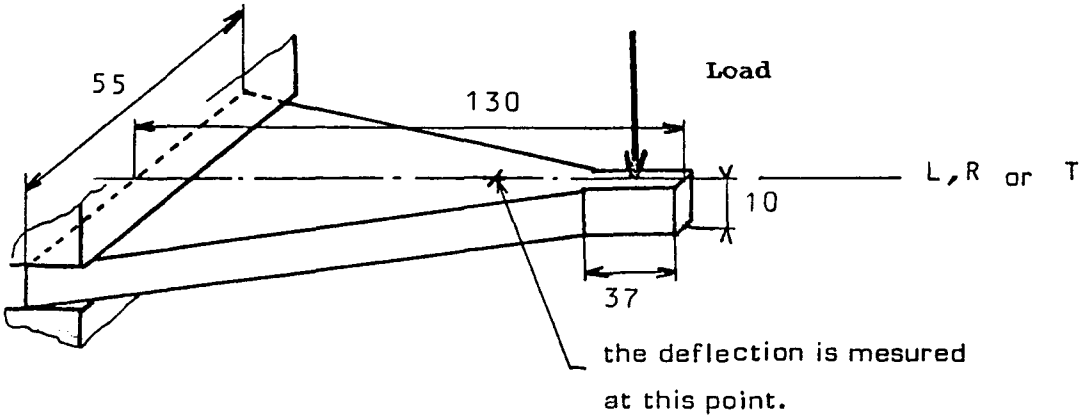

Figure 2 The isostress sample is tested in bending.

The increase in temperature allows us to observe the acceleration of creep when the temperature approached 100°C, but the same phenomena could be observed near to 50°C also. These events correspond to two different mechanisms, located by T_I and T_{II}. The important acceleration, due to mechanism I appeared in the four samples. Mechanism II was not observed on the dried sample (v_{f3} on the Fig. 6). The deflection curves versus temperature pointed out that the drying treatment decreased the temperature at which mechanism II appeared. As a matter of fact the instantaneous deflection (f_3 on the Fig. 6) of this sample was greater (+30%) than the others. Above 50°C, all the deflections converge toward the same value.

In order to compare these results with the literature, one must deduce from the answer at creep at increasing temperature, the couples $(1/T_0, \log f_0)$ of maxima of internal friction. Indeed, these couples are different from the couples $[1/T, \log(1/t)]$ in which t corresponds to the time when the maxima of creep speed was observed. A simple thermoactivated viscoelastic model[14,15] simulates the experimental answer and gives the characteristics of each mechanism: a relaxed rigidity, K_i; a time constant at 20°C, τ_i^{20}; an activation energy, ΔW_i.

Two strong assumptions are made in this model: (a) K_i is independent of the temperature and (b) Arrhenius's law governs the time constant:

$$\tau_i^{20} = \tau_i^{\infty} e \frac{\Delta W_i}{RT}$$

The precision of the values of the parameters is alas weak when the maximum of creep kinetic does not appear in the experimental window (mechanism I). Otherwise, the activation energy can be deduced from a single experiment, therefore the segments of a straight line can be drawn for each sample [Fig. 4(b)].

The relaxation of the most important amplitude (T_I), which is not completely included in our experimental window (20–100°C), is in the axe of the vitrous transition α of the PMMA. Mechanism II, with a weak amplitude, was not observed by other authors. Its existence must be confirmed by low-frequency experiments (10^{-3}, 10^{-4} Hz, 20°C).

Wood Samples

Figure 7 presents the compliance of the sample (s) and its increase (v_S) every 5 min:

$$\left.\begin{aligned} s &= \frac{\text{deflection}}{\text{load}} \\ vs &= \frac{\text{deflection}(t) - \text{deflection}(t-300)}{\text{load}} \end{aligned}\right\} \mu\text{m N}^{-1}$$

The curves are given in the three directions of orthotropy of wood (longitudinal, radial, and tangential) for three moisture contents. The moisture content influences the amplitude of a mechanism and the temperature at which it appears. The displacement of the two relaxations T_1 and T_0 in the experimental window are located by the sign T_i^H (relaxation i at the moisture content H). The curves agree with the assumption: The relaxed rigidity decreases when the moisture content increases.

For 30% of moisture content, we can clearly distinguish two relaxations T_1 and T_0 at the temperatures 50 and 80°C. For 10% of moisture content, T_1 and T_0 are slightly moved. Thus the temperature

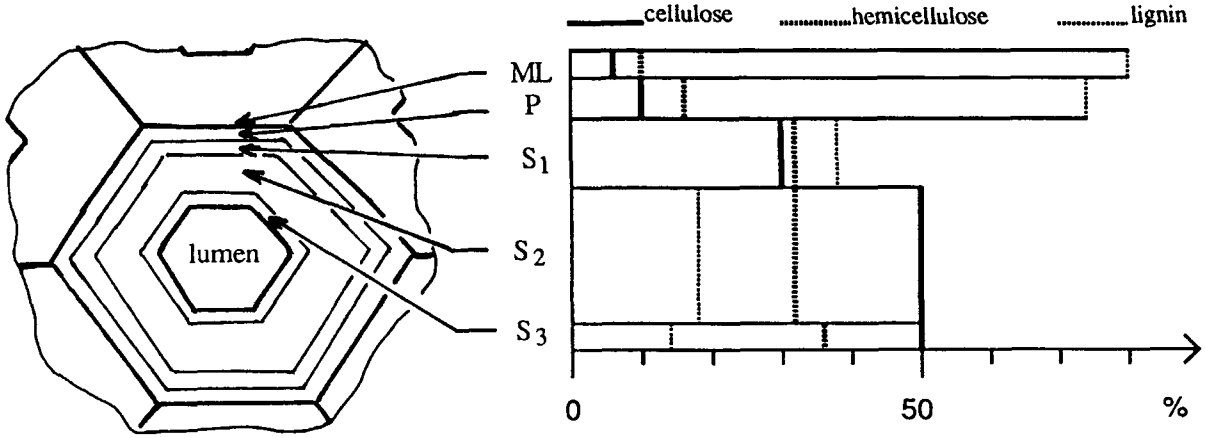

Figure 3 The polymeric composition of each layer of a wood fiber: ML, middle lamella; P, primary layer; S_{123}, secondary layers.

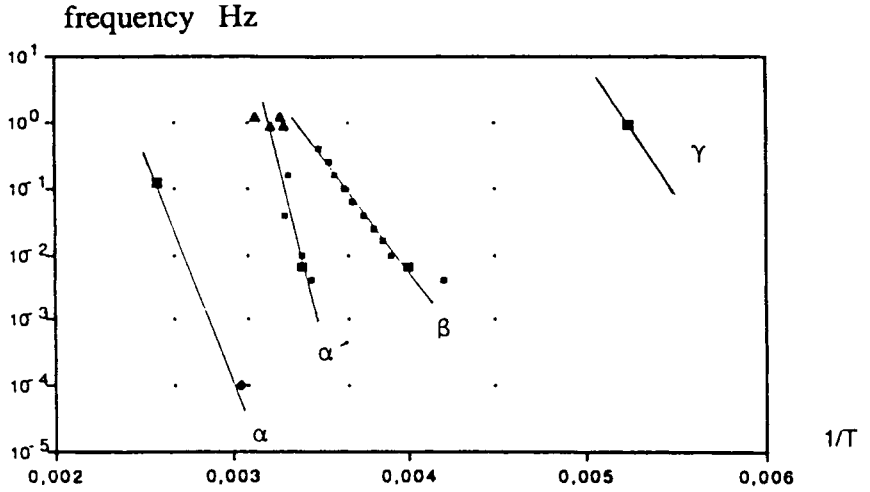

Figure 4a Position of the maximum of internal friction of PMMA in the correlation diagram from [5,2].

at which T_0 appears becomes greater than 100°C. The sensibility of T_1 and T_0 are even more important between the moisture contents 10 and 0%. At this last moisture content, the speed increases toward T_1 at 80°C, whereas one other relaxation T_{II} should approach 20°C.

The anisotropy of the relaxed rigidity of each relaxation are different: The relaxation T_1 appears weakly in the longitudinal direction and strongly in the radial and tangential ones. Therefore the relaxation T_0 is present in all three directions. The wood fiber is composed by several layers, which polymeric compositions are different (Fig. 3). The cause of T_1 must be located in the matrix (lignin, hemicellulose), and the cause of T_0 in the reinforcement (amorphous and semicrystalline cellulose). T_2

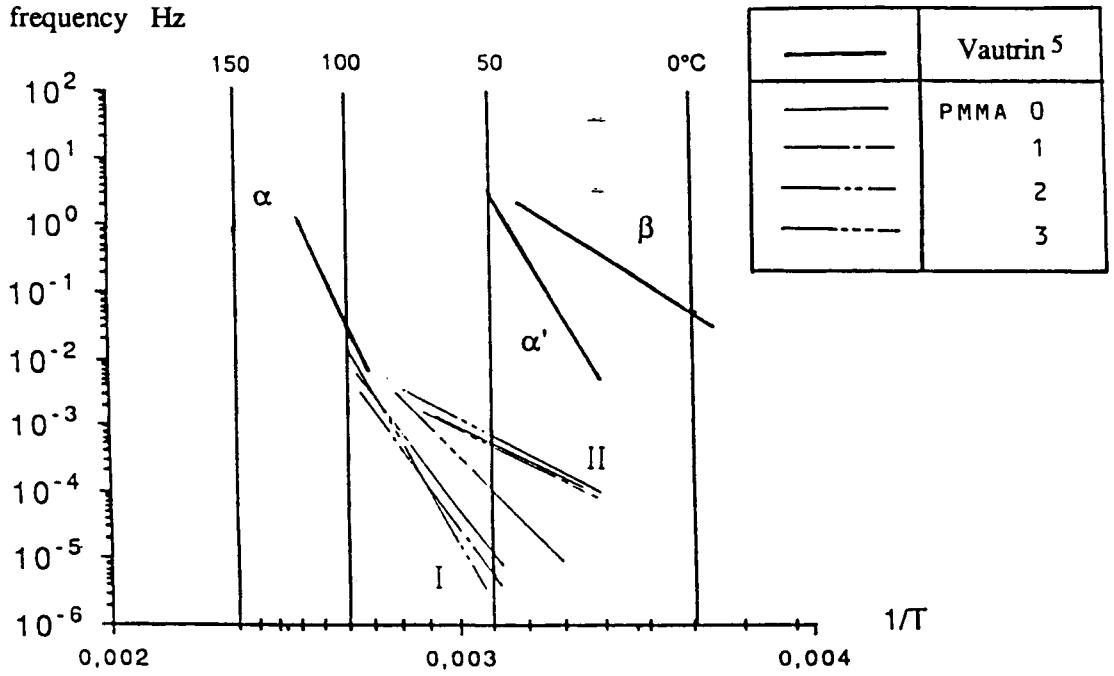

Figure 4b Position of the maximum of internal friction of PMMA, deduced from the creep at linearly increasing temperature.

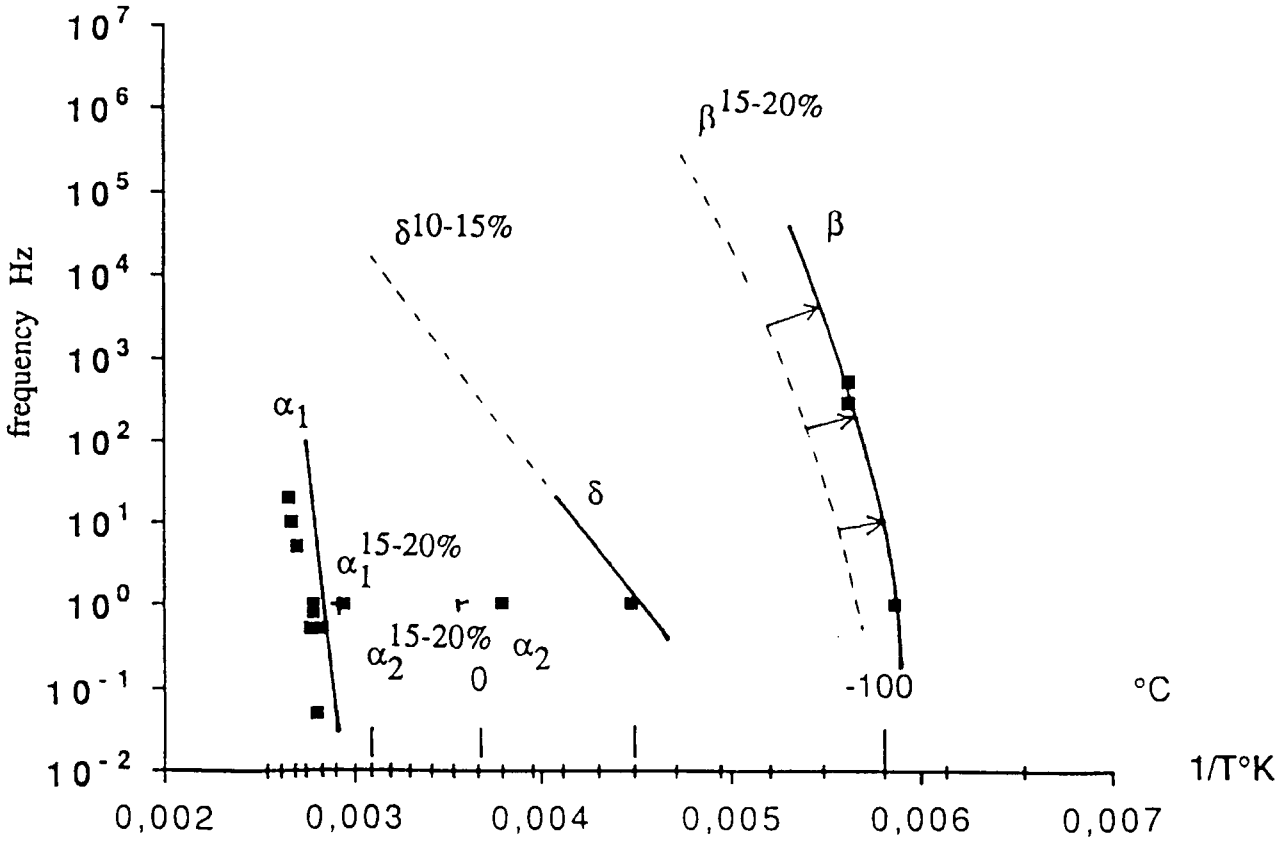

Figure 5a Position of the maximum of internal friction of Douglas wood in the correlation diagram for $10\% < H < 20\%$.

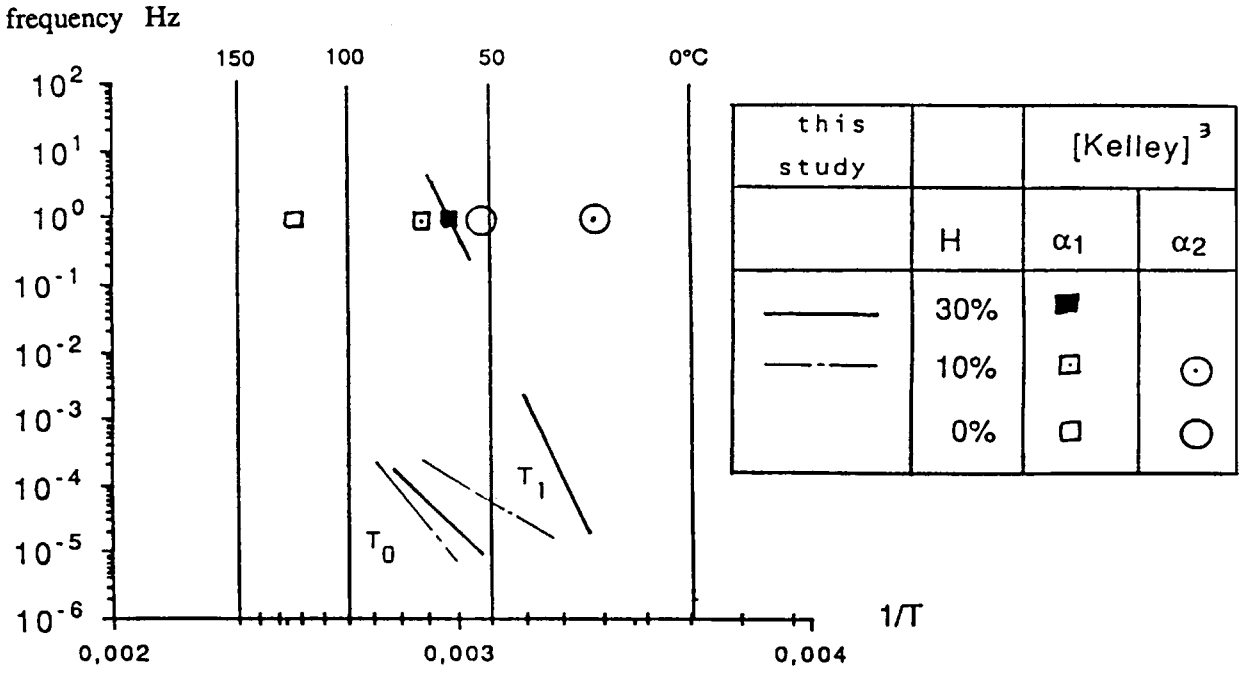

Figure 5b Position of the maximum of internal friction of Douglas wood, deduced from the creep at linearly increasing temperature.

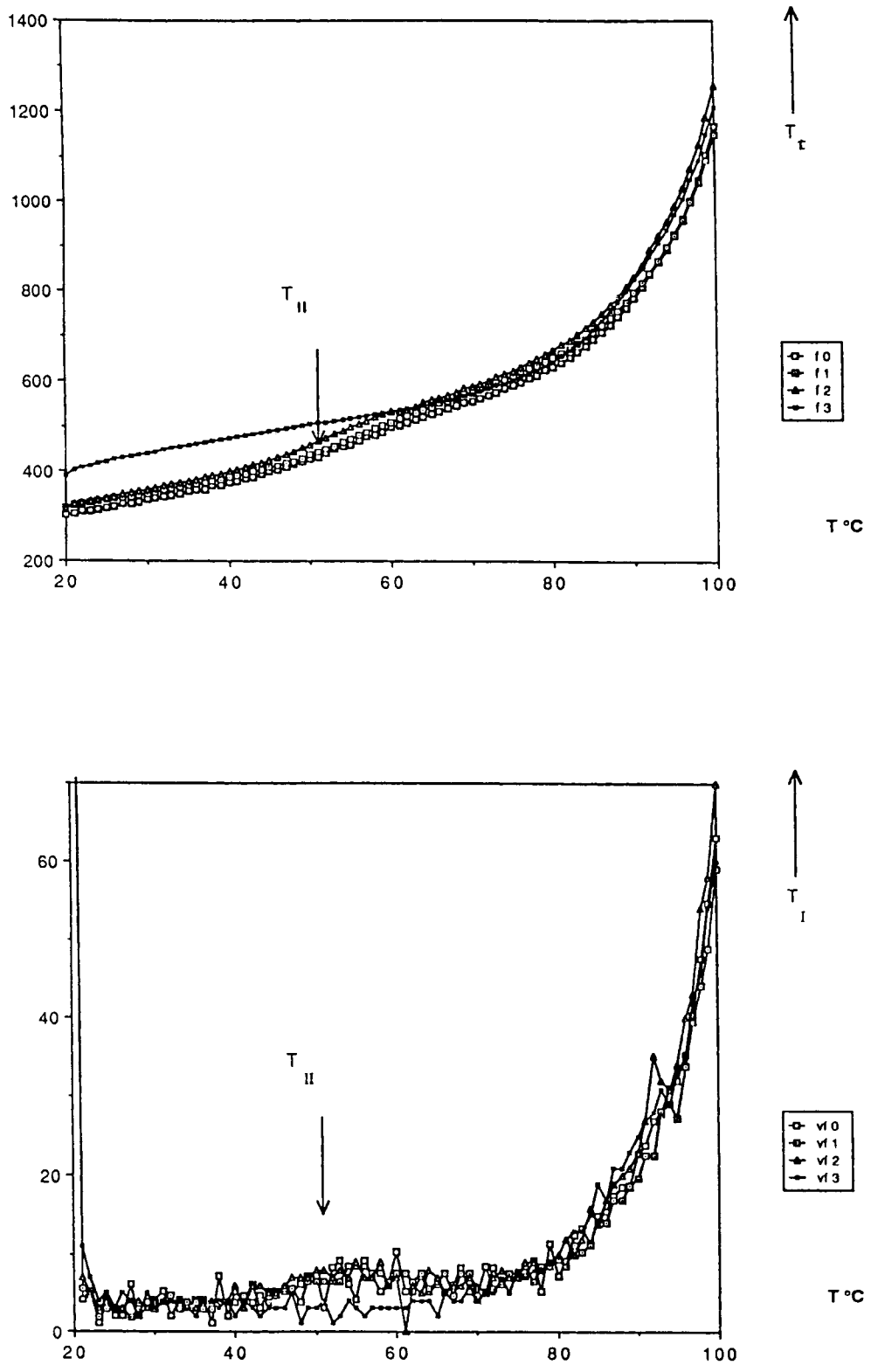

Figure 6 Evolutions of the deflection (f) and the creep speed (vf) with the temperature, for PMMA, during creep at linearly increasing temperature.

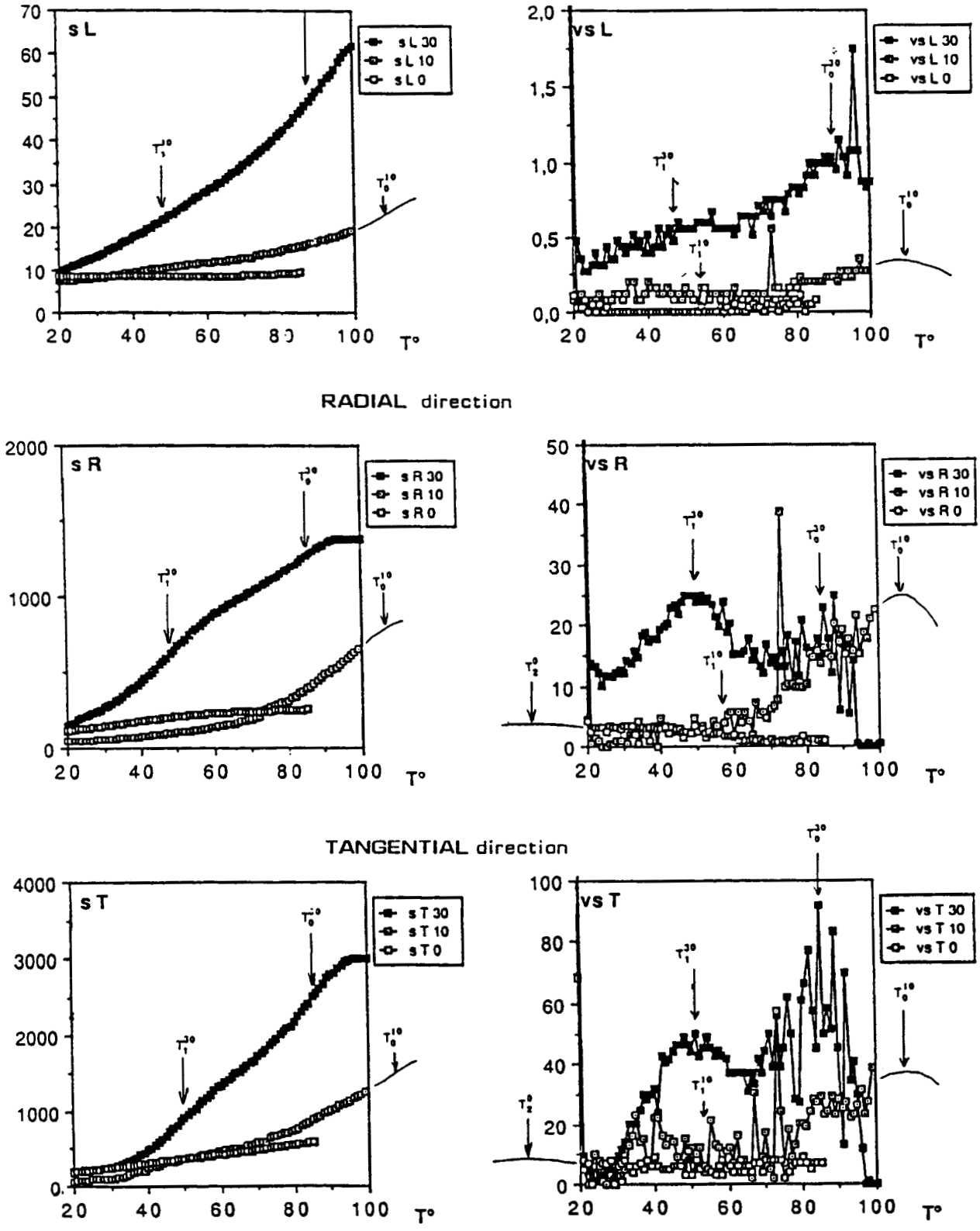

Figure 7 Evolution of the compliance of the wood samples with the temperature. SR 0: Compliance in the Radial direction for a moisture content H $\approx$ 0%; VSL30: Increase of compliance in the Longitudinal direction for a moisture content of H $\approx$ 30%.

should only appear in the radial and the tangential directions. We should notice that the relaxation T_0 appears systematically at a greater temperature (+7°C) in the longitudinal direction than in the other directions.

Our results are in good agreement with the literature[3] as it is shown by the correlation diagram of Figure 5(b) for a moisture content of 30%. T_1 is in the axis of the relaxation α_1; T_0 can not be observed at 1 Hz because the detection of its maximum of internal friction should require an experiment above 100°C. T_2 represents the approach of the relaxation α_2.

The difficulty in distinguishing T_1^{10} on the experimental curves (Fig. 7) induces an important incertitude on the position of the segment related to T_1 when $H \approx 10\%$ [Fig. 5(b)]. Nevertheless, the evolution to a higher temperature of this relaxation, when H decreases, is observed. T_2^0 does not belong to our experimental window: Its associated segment in the correlation diagram is obtained without precision, and it is not drawn.

CONCLUSIONS

The study of the delayed behavior of polymeric materials leads to a precision of the temperature and the frequency (eventually the moisture content) at which the experiments are undertaken. Using the correlation diagram, the evolutions of the mechanical characteristics (apparent modulus or internal friction) can be interpreted as the passing of several relaxations (vitrous or secondary transitions) in the tested zone in frequency and temperature. Thus the comparison with other results is easier.

The behavior at very low frequencies ($< 10^{-4}$ Hz) can be studied, using a creep experiment at linearly increasing temperature. This test allows observation in a single sample of mechanisms whose retarded time constant at 20°C varies from 10^3 s to several months, over a period of 6 h. If the maximum of creep kinetic is included in the experimental window, the activation energy, the time constant, and the amplitude of a mechanism can be evaluated.

In the case of an anisotropic materials such as wood, the anisotropy must be quantified for each mechanism: For wood, the anisotropy of the relaxed rigidity of the mechanism T_1 is different from those of the mechanism T_2. This fact allows us to localize in the matrix or in the fibers the relaxation concerned. The authors can thus point out the relaxation of the reinforcement of wood (cellulose) from a vitrous to a rubber state. This relaxation has never been observed, and it could be named α_0.

REFERENCES

1. Y. Wada and K. Yamamoto, *J. Phys. Soc., Jpn.*, **11,** 887 (1956).
2. G. M. Guerrin, Caractérisation en flexion quasistatique et dynamique d'un matériau thermo-hydro-viscoélastique: le bois, Thesis of the Institut Polytechnique of Lorraine, France, 1990.
3. S. S. Kelley, T. G. Rials, and W. G. Glasser, *J. Mat. Sci.*, **27,** 617 (1987).
4. W. G. Gall and N. G. Mc Crum, *J. Polym. Sci.*, **50,** 489 (1961).
5. A. Vautrin, Etude du comportement viscoélastique des solides par la méthode de traction modulée. Relaxations secondaires du polyméthyle méthacrylate, Thesis of Docteur Ingénieur of the Université of Nancy I, 1976.
6. M. Ziani and J. M. Genevaux, Proceedings of the 25th Conference of the Groupe Français de Rhéologie, Grenoble, 28–30 November 1990, France, Influence de l'humidité et de la température, sur les caractéristiques radiales et tangentielles du bois à basse fréquence.
7. J. M. Genevaux, Le fluage à température linéairement croissante: caractérisation des sources de viscoélasticité anisotrope du bois, Thesis of the Institut Polytechnique of Lorraine, 1989.
8. B. Lazan, *Damping of Materials and Members in Structural Mechanics,* Pergamon Press, Oxford (1968).
9. J. J. Aklonis and W. J. Macknight, *Introduction to Polymer Viscoelasticity,* Wiley-Interscience, New York.
10. C. C. Bauwens, *J. Mat. Sci.*, **8,** 968 (1973).
11. E. V. Thompson, *J. Polym. Sci.*, **6,** 433 (1968).
12. J. Bodig and B. A. Jayne, *Mechanics of Wood and Wood Composites,* Van Nostrand Reinhold, New York, 1982.
13. F. P. Kollmann and W. A. Cote, *Principles of Wood Science and Technology,* Vol. 1, *Solid Wood,* Springer-Verlag, Berlin, 1984.
14. J. M. Genevaux, Anisotropie du comportement différé: fluage sous température croissante d'un bois de peuplier, Proceedings of the conference "Comportement mécanique du bois," 1988.
15. J. M. Genevaux, "Fluage à température croissante: mise en évidence de transitions multiples" (available in english: "Anisotropy of the differed behaviour: creep at increasing temperature of a poplar wood"), Proceedings of the 23rd conference of the Groupe Français de Rhéologie, Bordeaux, 1988.

Received September 13, 1991
Accepted September 23, 1991